Chemical and Biological
Technologies in Agriculture
a SpringerOpen Journal

RESEARCH   **Open Access**

Humic matter elicits proton and calcium fluxes and signaling dependent on Ca^{2+}-dependent protein kinase (CDPK) at early stages of lateral plant root development

Alessandro C Ramos[1], Leonardo B Dobbss[2], Leandro A Santos[3], Mânlio S Fernandes[3], Fábio L Olivares[4], Natália O Aguiar[4] and Luciano P Canellas[4*]

Abstract

Background: The humic acid (HA) fraction of soil organic matter (SOM) exerts an effective plant growth promotion through a complex mechanism involving a coordinated activation of several key ion transport and signaling systems. We investigated the effects of HA on H$^+$ and Ca^{2+} cellular dynamics at the early stages of lateral plant root development.

Results: Emergence of lateral root in rice seedlings were related to specific H$^+$ and Ca^{2+} fluxes in the root elongation zone underlying an activation of the plasma membrane H$^+$-ATPase and of the Ca^{2+}-dependent protein kinase (CDPK). The latter was coupled with an increased expression of the voltage-dependent *OsTPC1* Ca^{2+} channels and two stress responsive CDPK isoforms, such as *OsCPK7* and *OsCPK17*.

Conclusions: HA act as molecular elicitors of H$^+$ and Ca^{2+} fluxes, which seem to be upstream of a complex CDPK cell-signaling cascade. These findings shed light on the first ion signaling events involved in the mechanism of action of HA on plant growth and development.

Keywords: Calcium ion; Anion channel; H$^+$-ATPase; Rice; Ion-selective vibrating probe; pH signaling; Physiological effects of humic substances

Background

Humic substances (HS) represent the major components of soil organic matter (SOM) and are complex supramolecular associations of biotically and abiotically transformed biomolecules released in soil after cell lyses [1]. They exert diverse morphological, physiological, and biochemical influence on plant growth [2]. HS effects may be either stimulating or inhibiting plant activities, depending on their origin, molecular composition, and concentration, and also varying with plant species and interactions with symbiotic microorganisms [3]. Despite prolonged efforts aimed to correlate molecular composition and structural arrangements of humic substances

with their biological activity on higher plants, the involved mechanisms of action are yet to be elucidated [4-7].

Tip-growing plant cells, as root hair and cells in elongation zone, exhibit markedly polarized internal gradients and/or external fluxes of important regulatory ions (e.g., calcium, protons, and anions). Calcium (Ca^{2+}) ions are since long recognized to represent important second messengers in many signaling pathways, while increasing evidences have accounted pH changes to several Ca^{2+}-dependent signal transduction in plant and fungal cells [8,9].

Protons (H$^+$) are major contributors to cell currents [10] and H$^+$ fluxes through membranes control the cytosolic pH regulation, the secondary active transport of organic and inorganic nutrients, turgor-regulation, and cell wall plasticity. These processes are described by the 'acid-growth theory' [11] that suggests a close relationship

* Correspondence: canellas@uenf.br
[4]Universidade Estadual do Norte Fluminense Darcy Ribeiro (UENF) Núcleo de Desenvolvimento de Insumos Biológicos para Agricultura (NUDIBA), Av. Alberto Lamego 2000, Campos dos Goytacazes 28013-602, Brazil
Full list of author information is available at the end of the article

Ramos *et al. Chemical and Biological Technologies in Agriculture* (2015) 2:3

Page 2 of 12

between H^+ pump activity and wall acidification and cell expansion. This mechanism has been also associated with the auxin effects on seed embryo growth [12] and early growth responses to gravistimulation of root cells [13].

Auxin cell signaling elicited by HS was previously showed by Trevisan et al. [14] using the *DR5::GUS* construct in *Arabidopsis*, and evidence for their involvement in plasma membrane H^+-ATPase activation has been recently reported [7,15]. This enzyme creates the electrochemical gradient of H^+ that energizes secondary transport processes, including ion and nutrient uptake [16]. The influence of HS on H^+-ATPases and H^+ transport has been extensively reported [17,18].

Protein kinases have also paramount importance in cell signal transduction [19,20]. They are responsible for the post-translational control of target proteins and act as critical regulators of various signaling cascades [19]. Furthermore, many plant receptors are endowed with protein kinase activity, through the participation in processes like growth, hormone perception, and stress responses [21]. Cytoplasmic Ca^{2+} oscillations also play a key role in cell signaling, either through activation of ion channels or as secondary messenger [22]. Signaling occurs when the cell is stimulated to release the Ca^{2+} ions stored in intracellular compartments, or when Ca^{2+} ions enter the cell via the plasma membrane, resulting in cytosolic waves in which the Ca^{2+} concentration increases by 1 or 2 orders of magnitude over a short period of time [22,23].

The aim of this work was to verify whether humic matter is capable to regulate the elongation of lateral roots in rice seedlings by a mechanism of integrated modulation of membrane Ca^{2+} and H^+ fluxes and specific calcium-dependent protein kinase (CDPK) activations.

Methods

Isolation of humic acids from vermicompost
A vermicompost was obtained from cattle manure. The organic residues were mixed and earthworms were added at a ratio of 5 kg earthworms (*Eisenia foetida*) per m^3 of organic residue. A bed of worms and organic residues was first prepared in a container and additional layers of organic residues were periodically placed over the pile, as a function of temperature, until the pile reached 50 cm. At the end of the transformation process (3 months after addition of the last organic residues), worms were transferred into a pile of fresh organic residue (plant + cattle manure) placed in a corner of the container and the vermicompost removed and sieved through a 2-mm sieve. The vermicompost had the following properties: pH 7.8, 46.5 g kg^{-1} total organic carbon and 17.3 g kg^{-1} humic acid (HA) carbon. HA were isolated from vermicompost and purified as reported elsewhere [17]. The

HA were suspended in distilled water and titrated to pH 7.0 by automatic titrator (VIT 909 Videotitrator, Copenhagen, Denmark) with a 0.1 NaOH solution under N2. The resulting sodium-humates were then passed through a 0.45-μm Millipore filter (Millipore, Billerica, MA, USA), dialyzed against ultrapure water and freeze-dried.

HA characterization
Total organic carbon (OC), nitrogen (TN), and hydrogen (H) contents were determined by dry combustion using an automatic CHN analyzer (Perkin-Elmer 2400 Series, Perkin-Elmer, Norwalk, CT, USA). The oxygen (O) content was obtained by difference after deducting the ash content (2.1%). The C functionality distributions of the humic acid samples were determined by solid-state CP-MAS ^{13}C-NMR spectroscopy. The spectra were acquired with an Avance 500 MHz (Bruker, Karlsruhe, Germany) spectrometer equipped with a 4-mm-wide bore MAS probe and operating at ^{13}C and ^{1}H frequencies of 125 MHz and 500 MHz, respectively. The samples (100 to 200 mg) were packed in 4-mm zirconia rotors with Kel-F caps, which were spun at 13 ± 1 kHz. The spectra were acquired by the ramped CP-MAS method, with linear amplitude variation of the ^{1}H pulse. The experiments were carried out using a cross-polarization time of 1.0 ms, an acquisition time of 25 ms, a cycle delay of 2 s and a high-power two-pulse phase modulation (TPPM) proton decoupling of 70 KHz. The Bruker Topspin 1.3 software (Bruker Biospin, Karlsruhe, Germany) was used to collect and process the spectra. All the free induction decays (FIDs) were transformed by applying a 4 k zero filling and a line broadening of 75 Hz. The spectra were normalized by area and integrated in the following ^{13}C chemical shift intervals: 190 to 160 ppm (carbonyls of ketones, quinones, aldehydes, and carboxyls), 160 to 140 ppm (phenols and O-substituted aromatic C), 140 to 110 ppm (unsubstituted aromatic C and olefinic C), 110 to 95 ppm (anomeric C), 95 to 65 ppm (O-alkyl systems), 65 to 45 ppm (methoxy substituent; N-alkyl groups), and 45 to 0 ppm (alkyl C, mainly CH_2 and CH_3). The relative areas of the alkyl (45 to 0 ppm) and aromatic (160 to 110 ppm) components were summed to represent the proportion of hydrophobic C in the humic samples (degree of hydrophobicity, HB). Similarly, the summation of the relative areas in intervals related to polar groups (190 to 160 ppm and 110 to 45 ppm) indicates the degree of C hydrophilicity (HI); the HB/HI ratio was then calculated.

Germination of *Oryza sativa*
Rice (*O. sativa* var. Nipponbare) seeds provided by Plant Mineral Nutrition Laboratory of UFRRJ, were surface sterilized by soaking in 0.5% (*w/v*) NaClO for 30 min, followed by rinsing and then soaking in water for 6 h. Afterward, the seeds were sown on wet filter paper and

Ramos *et al. Chemical and Biological Technologies in Agriculture* (2015) 2:3

Page 3 of 12

germinated in the dark at 28°C. A preliminary assay was conducted by using 4-day-old seedlings with roots approximately 5 cm long. These were transferred into a solution containing 2 mM CaCl2 and HA at varying concentrations: 0, 0.5, 1.0, 2.0, 4.0, 6.0, and 8.0 mM C L^{-1}. A minimal medium (2 mM CaCl2) has been used to avoid any interference from nutrients that may act synergistically with humic matter on plant growth and metabolism. After regression analysis, a new experiment was carried out using the best concentration (best dose = 3.5 mM).

Root growth measurement
On the 7th day, 20 seedling roots for each treatment were collected to estimate root area using Delta-T scan software (Delta-T Devices, Cambridge, UK).

Frequency of sites of lateral root emergence
Seeds of rice were germinated for 4 days in wet filter paper and rooted in a medium containing 0 or 3.5 mM C HA L^{-1}. The whole root systems (three replicates) of both treatments were harvested every day during a period of 7 days to evaluate the number of mitotic sites after mild digestion by boiling at 75°C for 20 min in KOH (0.5%, *w/v*) and hematoxylin treatment according to Canellas et al. [17].

PM-enriched vesicles
Plasma membrane (PM) vesicles were isolated from rice roots grown with and without 3.5 mM C HA L^{-1} using differential centrifugation. In brief, about 15 g (fresh weight) of rice roots was homogenized using a mortar and pestle in 30 mL of ice-cold buffer containing 250 mm Suc, 10% (*w/v*) glycerol, 0.5% (*w/v*) polyvinylpyrrolidone-40 (40 kD), 2 mM ethylenediaminetetraacetic acid (EDTA), 0.5% (*w/v*) bovine serum albumin, and 0.1 M Tris-HCl buffer, pH 8.0. Just before use, 150 mM KCl, 2 mM dithiothreitol (DTT), and 1 mM phenylmethylsulfonyl fluoride were added to the buffer. The homogenate was strained through four layers of cheesecloth and centrifuged at 8,000×*g* for 10 min. The supernatant was centrifuged once more at 8,000×*g* for 10 min and then at 100,000×*g* for 40 min. The pellet was resuspended in a small volume of ice-cold buffer containing 10 mM Tris-HCl (pH 7.6), 10% (*v/v*) glycerol, 1 mM DTT, and 1 mM EDTA. The suspension containing membrane vesicles was layered over a 20%/30%/42% (*w/w*) discontinuous Suc gradient that contained, in addition to Suc, 10 mM Tris-HCl buffer (pH 7.6), 1 mM DTT, and 1 mM EDTA. After centrifugation at 100,000×*g* for 3 h in a swinging bucket, the vesicles that sedimented at the interface between 30% and 42% (*w/w*) Suc were collected, diluted with three volumes of ice-cold water, and centrifuged at 100,000×*g* for 40 min. The pellet was resuspended in a buffer containing 10 mM Tris-HCl

(pH 7.6), 10% (*v/v*) glycerol, 1 mM DTT, and 1 mM EDTA. The vesicles were either used immediately or frozen under liquid N2 and stored at –70°C until use. Protein concentrations were determined by the method of Lowry et al. [24].

ATPase activity
ATPase activity in PM vesicles was determined by measuring the release of Pi colorimetrically. Between 80% and 95%, ATPase activity in PM vesicles, as measured at pH 6.5, was inhibited by vanadate (0.1 mM), a very effective inhibitor of the PM P-type H$^+$-ATPase. In all experiments, the ATPase activity was measured at 30°C, with and without vanadate, and the difference between these two activities was attributed to the PM H$^+$-ATPase.

ATPase H$^+$ pumping
The electrochemical H$^+$ gradient generated by the H$^+$-ATPase was estimated from the initial rate of quenching of the fluorescent pH probe 9-amino-6-chloro-2-methoxyacridine (ACMA) (2.5 µM, 415/485 nm excitation/emission) and expressed in percentage of quenching per minute. The assay medium contained 10 mM HEPES-KOH (pH 6.5), 100 mM KCl, 3 mM MgCl2, 2.5 µM ACMA, and 0.05 mg L^{-1} PM vesicle proteins. The reaction was triggered by addition of 1 mM ATP.

Measurements of H$^+$ and Ca^{2+} anion fluxes
Measurements of ion fluxes in rice plants treated with HA were conducted by using the ion-selective vibrating probe system. For H$^+$ and Ca^{2+} measurements, rice roots were grown in hydroponic conditions and placed in plastic Petri dishes (140 × 140 mm) filled-up with 30 mL of modified Clark solution at ¼ strength supplemented with 0 mM or 3.5 mM C HA, excepted for Ca^{2+} measurements when 100 µM Ca^{2+} was used. Three to four days after germination, ion fluxes were analyzed by the vibrating probe system. H$^+$-specific vibrating microelectrodes were produced as described by Feijó et al. [8]. Micropipettes were pulled from 1.5-mm borosilicate glass capillaries with a Sutter P-98 Flaming Brown electrode puller (www.sutter.com). These were then baked in covered dishes at 250°C for 8 to 12 h and vaporized with dimethyl dichlorosilane (Sigma, St. Louis, MO, USA) for 30 min, and the covers were removed before further baking at 250°C for 1 h. After silanization, the capillaries were backfilled with a 15- to 20-mm column of electrolyte (15 mM KCl and 40 mM KH$_2$PO$_4$, pH 6.0 for H$^+$; 100 mM KCl for anions; 100 mM CaCl$_2$ for Ca^{2+}) then front-loaded with a 20- to 25-µm column of a pH selective liquid exchange cocktail from Fluka (Milwaukee, WI, USA). This contained protons (hydrogen ionophore II-cocktail B, no. 95223), chloride (chloride ionophore cocktail A, no 24902), and calcium (calcium ionophore I

Ramos *et al. Chemical and Biological Technologies in Agriculture* (2015) 2:3

Page 4 of 12

cocktail A, no 21048). This solution was drawn into the tip of the microelectrode by application of suction to the basal end of the pipette. We used Cl^- electrodes to measure the anion fluxes, although this electrode has poor selectivity for Cl^- under our experimental conditions. According to Messerli et al. (2004), 1 mM NO_3 is enough to diminish the Cl^- selectivity. Indeed, under low Cl^- concentration, Cl^- detection was influenced by NO_3^-, SO_4^{2-} and PO_4^{2-}, suggesting a low selectivity of this ionophore under our experimental conditions. The Cl^- electrode calibration with different anions also showed that this electrode could detect NO_3^- but not SO_4^{2-} and PO_4^{2-}. Therefore, our measurements reflected changes in the 'anionic' concentration rather than in Cl^- fluctuations. An Ag/AgCl wire electrode holder (World Precision Instruments, Sarasota, FL, USA) was inserted into the back of the microelectrode in order to establish electrical contact with the bathing solution. The ground electrode was a dry reference (DRIREF-2, World Precision Instruments) that was inserted into the sample bath. In order to obtain a calibration line, microelectrodes were calibrated at the beginning and end of each experiment using standard solutions covering the experimental range of each ion. Both the slope and intercept of the calibration line were used to calculate the respective ion concentration from the mV values measured during the experiment near and distant from the root surface. A detailed description of the ion-selective vibrating probe system was reported by Feijó et al. [8] and Ramos et al [25,26]. The vibrating-electrode system was attached to a Nikon Eclipse TE-300 inverted microscope (Nikon, Melville, NY, USA) and housed inside a copper-sheet Faraday cage over a vibration-free platform. For routine experiments, an X20 Plan Apo objective under differential interference contrast (DIC) was used.

Kinase activity assays

Protein kinase activity was measured by incorporating radioactive phosphate from ATP into syntide 2 (Sigma) [27]. Protein kinase activity was assayed in 20 µl of 30 mM Hepes-Tris buffer (pH 7.0), 2.5 mM free Mg^{2+}, 1.5 mM EGTA and 1.5 mM N-hydroxyethylethylenediaminetriacetic acid (HEDTA), 10 µM free Ca^{2+}, 50 µM syntide 2, and 0.2 mM [γ-32P]ATP (3.77 TBq mol^{-1} from Amersham Bioscience (Piscataway, NJ, USA), unless stated otherwise). Reactions were started by adding 1 µl of a kinase-containing solution and incubated for 30 min at room temperature. At the end of incubation, the reaction mixture was spotted on 2 cm × 2 cm Whatman P81 phosphocellulose paper pieces. These were then washed three times with 75 mM H3PO4 (for 10 min), rinsed for 5 min in ethanol, air dried, placed in vials with scintillation liquid and levels of radioactivity determined.

Rice growth conditions for gene expression experiment

Rice plants was held in a growth chamber, with a light cycle of 12/12 h (light/dark), photosynthetic photons flux of 400 µmol m^{-2} s^{-1}, relative humidity of 70%, and temperatures of 28°C/24°C (day/night). Rice seeds (*O. sativa* L. cv. Nipponbare) were previously disinfected in 2% sodium hypochlorite solution for 15 min and then washed several times with distilled water. These seeds were germinated only in distilled water. Five days after germination, the seedlings were transferred to 0.3 liter pots, where five plants per pot received Hoagland solution modified to contain 1/4 of the total ionic strength and 1.5 mM of N (1.25 mM NO_3^--N and 0.25 mM NH_4^+-N) pH 5.8. This nutrient solution was replaced every 2 days. Thirteen days after germination, the plants received the same solution with or without humic acid (3.5 mM of C). The experiment was conducted in a completely random design with three replications. Root samples were collected at 24 h for total RNA extraction and real-time PCR.

Total RNA extraction and cDNA synthesis

Total RNA was extracted according to Gao et al. [28] with modifications using NTES buffer (0.2 M Tris-HCl pH 8.0; 25 mM EDTA; 0.3 M NaCl; 2% SDS). Three root samples were ground in N_2 and homogenized in a mixture containing 1 mL NTES buffer and 0.7 mL of phenol: chloroform (1:1). Homogenized samples were centrifuged at 18,000×*g* for 20 min at 4°C and each supernatant transferred to a new tube. Total RNA was precipitated by adding 1/10 volume of 3 M sodium acetate pH 5.2 ($NaOAc_{DEPC}$) and one volume of cold isopropanol. Samples were placed at −80°C for 1 h and centrifuged at 18,000×*g* for 20 min after that time. Pellets were re-suspended in 0.5 mL of H_2O_{DEPC} and precipitated overnight at 4°C by the addition of 0.5 mL of 6 M lithium chloride ($LiCl_{DEPC}$). After centrifugation at 18,000×*g* for 20 min, pellets were re-suspended with 0.5 mL H_2O_{DEPC} and precipitated again with addition of 0.5 mL LiCl 6 M for 1 h on ice. After centrifugation at 18,000×*g* for 20 min, pellets were re-suspended in 0.5 mL of H_2O_{DEPC}, precipitated with two volumes of ethanol for 1 h at −80°C and washed with 70% ethanol. The pellets were dried on ice for 10 min and dissolved in 30 µL of H_2O_{DEPC}.

The quality of total RNA extracted was verified spectrophotometrically through A_{260}/A_{230} and A_{280}/A_{260} ratios and visualization in agarose gel (1%) with ethidium bromide. Total RNA samples used for cDNA synthesis were treated with DNAse I (Invitrogen, Inc., Waltham, MA, USA) by following the manufacturer's instructions. Single strand cDNA was synthesized by using the 'TaqMan Reverse Transcription Reagents' (Applied Biosystems, Inc., Loughborough, UK) and oligo dT primer according to the manufacturer's instructions.

Ramos *et al. Chemical and Biological Technologies in Agriculture* (2015) 2:3

Page 5 of 12

Real-time PCR

Real-time PCR reactions were performed in duplicate, using 'SYBR® Green PCR Master Mix' kit (Applied Biosystems, Inc.) according to the manufacturer's instructions. PCR reactions were as follows: 10 min at 95°C, 45 amplification cycles at 95°C for 15 s and 60°C for 1 min (annealing, extension, and fluorescence detection), followed by the 'melting curve' in order to verify the specificity of the reaction. Actin gene (NM 001057621.1) was used as an endogenous control. The primer sequences for *OsCPK7*, *OsCPK17*, and *OsTPC1* were designed with Primer Express software (Applied Biosystems) (Additional file 1: Table S1) and OsA7 [29]. The specificity of the primer sequences was analyzed using BLAST at TIGR (http://rice.plantbiology.msu.edu/) and in NCBI (http://www.ncbi.nlm.nih.gov) as well as experimentally at the end of the PCR reaction through the melting curve. Relative expression was performed according to Livak and Schmittgen [30], using the nutrient solution without humic acid as reference.

Results

HA characterization

The C content of the HA was 44.7%, whereas N and H content were 3.51% and 5.36%, respectively. The ^{13}C CPMAS NMR spectrum of HA is shown in supplementary data (Additional file 2). It was characterized by strong signals in the O-alkyl-C (56 to 110 ppm) and alkyl-C (45 to 0 ppm) regions, revealing a molecular composition dominated by carbohydrates and aliphatic components. The signals related to O-Alkyl-C and alkyl-C components represent in fact the majority of the total organic C, accounting respectively for the 40.9% and 21.9% of the total area of the spectra. The different resonances in the O-alkyl-C region (56 to 110 ppm) are currently assigned to monomeric units in oligo- and polysaccharidic chains of plant tissues. The signal centered at 72 ppm corresponds to the overlapping resonances of carbons 2, 3, and 5 in the pyranoside structure in cellulose and hemicellulose. These signals may represent the di-O-alkyl carbon of polysaccharidic chains other than cellulose such as the hemicellulose components contained in cell wall of the vascular tissues, like xylan, glucomannas, etc. Moreover, the shoulders around 20/23 ppm could be assigned to the methyl group in acetyl substituent in hemicellulose components.

The broad peak in the Alkyl-C region (30 ppm) of NMR spectra indicated the presence of alkyl chains (-CH$_2$- groups) derived mainly from various lipid compounds, plant waxes, and plant polyesters like cutin and suberin. The main signal at 56 ppm may be associated with either the methoxyl substituent on aromatic rings of guaiacyl and syringyl units in lignin, or with C-N bonds in amino acid moieties. The broad band around 131 ppm may be mainly related to unsubstituted and C-substituted phenyl carbons of lignin monomers of guaiacyl and syringyl units as well as to condensed aromatic moieties, while the signals shown in the phenolic aromatic region (152 ppm) indicated the presence of O-substituted ring carbon derived from different aromatic structures. The resonances included in the 148 to 155 ppm chemical shift range are in fact usually assigned to carbons 3, 4, and 5 in the aromatic ring in lignin components, carbons 3 and 5 being coupled to methoxyl substituents (see Additional file 2: Figure S1. However, the prominent peak found at 145 and 157 ppm in the NMR spectra, suggest also the presence of tannin derivatives. The aromatic carbon represents 27.9% of spectrum. Finally, the broad signal at 174 ppm (8.3%) indicates the content of carbonyl groups of aliphatic acids and amino acid moieties, as well as that of acetyl groups in hemicellulose components.

Root growth promotion by HA

A quadratic model ($R^2 = 0.95$, $P < 0.001$) describes the effects of different concentrations of HA on number of lateral roots emerged from rice seedlings (Figure 1). The optimal concentration of HA on a carbon content basis was 3.5 mM. The quantitative results of root area and number of mitotic sites were normalized in respect to control. The elongation/differentiation zone of the root includes small, densely meristematic cells in continuous metabolic activity that is more susceptible to lateral root formation. A marked effect was observed on root surface area after exposure to HA (data not shown).

HA effect on H$^+$-ATPase activity

Treatment of PM vesicles isolated from rice roots for 7 days with 3.5 mM C HA L^{-1} produced an increase in vanadate-sensitive ATP hydrolysis (Figure 2A) as well as a steeper ATP-dependent proton gradient, as measured by quenching of ACMA fluorescence (Figure 2B). The initial rate of gradient formation and ATP hydrolysis were enhanced by two- to threefold in response to treatment with HA.

HA effects on H$^+$, Ca^{2+} and anion fluxes, and on CDPK

Analysis of the root H$^+$ flux rate using a noninvasive technique revealed a differential pattern of H$^+$ fluxes along the lateral rice roots when treated with HA (Figure 3A). In HA-treated rice roots, apical (0 to 100 μm), meristematic (100 to 300 μm), and elongation (300 to 800 μm) zones showed a considerable increase on H$^+$ efflux if compared to the apex zone. In contrast, the control roots presented strong H$^+$ influxes (Figure 3A). A sixfold stimulation on H$^+$ effluxes was observed at the elongation zone in the presence of 3.5 mM C HA ($P < 0.001$), that resulted in the lowest root surface pH value (Figure 3B). These superior H$^+$ effluxes found at the

Ramos *et al. Chemical and Biological Technologies in Agriculture* (2015) 2:3
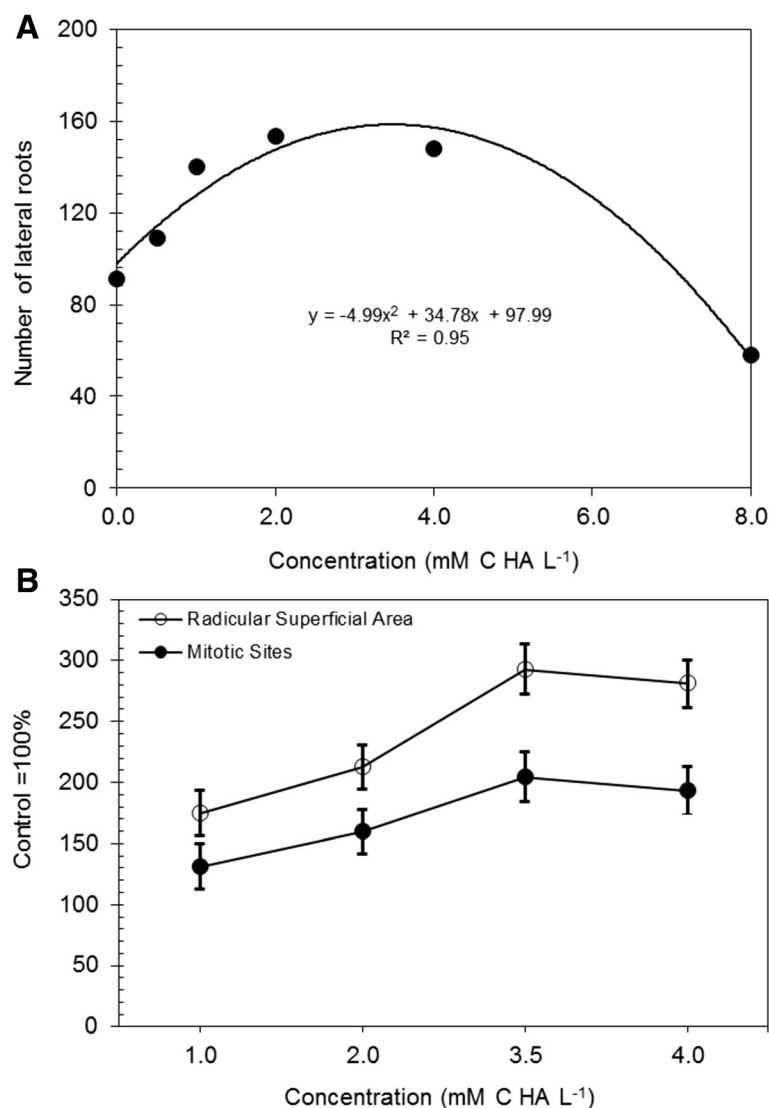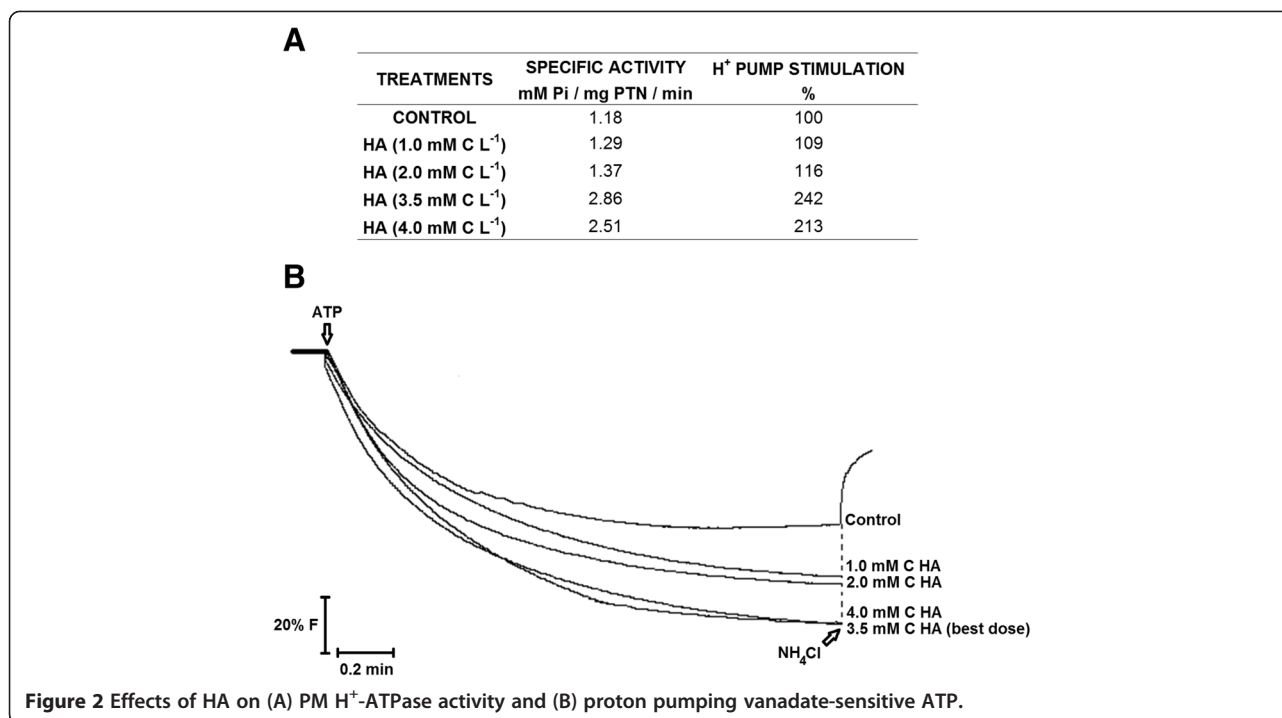
Page 6 of 12

Figure 1 Effect of different HA concentrations on number of lateral roots which emerged from principal axis (A). Data are the mean of 25 rice seedlings. **(B)** radicular superficial area and number of mitotic sites.

elongation zone of HA-treated roots were vanadate-sensitive which suggests the H^+-ATPase activity triggers ion dynamics in the presence of HA (Figures 2 and 3A).

Patterns of the Ca^{2+} fluxes in the control and HA-treated roots revealed a quite different scenario. Treatment with HA also increased Ca^{2+} influxes at the elongation zone (Figure 4), thus leading to a possible increase in free cytosolic Ca^{2+} concentration. At such root zone, a negative correlation can be observed between Ca^{2+} and H^+ ion fluxes ($r = -0.8951$ $P < 0.001$). On the other hand, a significant (tenfold) increase in anion efflux was observed in all root zones of rice seedlings treated with HA (Figure 5). Furthermore, we observed a clear effect of HA on the enhancement of CDPK activity in the experiments described here (Figure 6).

Relative gene expression of Ca^{2+} channels (OsTPC1), PM H^+-ATPase (OsA7), and calcium-dependent protein kinase (OsCPK7 and OsCPK17)

To address the aforementioned increase in Ca^{2+} efflux, we examined the expression level of *OsTPC1* voltage-dependent Ca^{2+} channel in rice seedlings at the early stage of HA treatment. OsTPC1 encoded a putative voltage-gated Ca^{2+} channel from rice, ubiquitously expressed in mature leaves, shoots, and roots [31]. In a study for functional characterization of *OsTPC1*, Kurusu et al. [31] suggested that OsTPC1 has Ca^{2+} transport activity across the plasma membrane and is involved in the regulation of growth and development in rice. *OsTPC1* significantly increased upon HA treatment in respect to control plants (Figure 7D). In addition, we observed a concomitant

Ramos *et al. Chemical and Biological Technologies in Agriculture* (2015) 2:3

Page 7 of 12

A

TREATMENTS	SPECIFIC ACTIVITY mM Pi / mg PTN / min	H⁺ PUMP STIMULATION %
CONTROL	1.18	100
HA (1.0 mM C L⁻¹)	1.29	109
HA (2.0 mM C L⁻¹)	1.37	116
HA (3.5 mM C L⁻¹)	2.86	242
HA (4.0 mM C L⁻¹)	2.51	213

B

Figure 2 Effects of HA on (A) PM H^+-ATPase activity and (B) proton pumping vanadate-sensitive ATP.

enhancement of *OsA7* PM H^+-ATPase expression in rice seedlings treated with HA (Figure 7C). The *OsA7* isoform is a highly expressed PM H^+-ATPase member of the subfamily II [32]. Sperandio et al. [29] showed that *OsA7* is upregulated in response to nitrogen resupply and suggested that *OsA7* could be involved in N nutrition in rice. We also evaluated the expression of two CDPK genes, *OsCPK7* and *OsCPK17*, both constitutively expressed in roots, stems, leaves, and panicles and responsive to various stress stimuli [33]. *OsCPK7* was upregulated by salt stress in roots [33], jasmonic acid [34], cold, and gibberellin [35] and suppressed by rice blast infection [33]. *OsCPK17* is downregulated by cold, drought, and salt stress in the rice seedlings [33]. Both *OsCPK7* and *OsCPK17* showed an increase of expression at 24 and 72 h after HA treatment as compared to untreated plants (Figure 7A,B).

Discussion

We used in this study a humic acid-like substance extracted from a vermicompost obtained from cattle manure with a large presence of OCH_3 groups with NMR spectral resonance at 56 ppm (Additional file 1) that is a trait for promotion of lateral root emergence, as shown previously [36]. The best dose-response concentration for lateral root induction of rice plantlets was used (Figure 1), and it was found that the HA treatment changed ion fluxes pattern over the root axis. Such changes for H^+ efflux was well characterized by other research reports which used using molecular and biochemical approaches involving H^+-ATPase enzymatic activity measurements

to establish a relation with HA bioactivity in plants [2,3,7,15,17]. Here, using a vibration probe device, we specifically detected and unequivocally showed live H^+ flux over different anatomical regions of the rice root axis displayed by the presence of HA (Figure 3A).

In comparison with control, the largest rates of H^+ efflux coupled with acidic surface pH following the HA treatments were located at the elongation/differentiation zones of rice roots, where plant cells with increased growth rates (reflected by cell volumetric expansion) and large cell differentiation are found (Figure 3). As quoted in literature, these effluxes are dependent on PM H^+-ATPase (PMA) activity (Figure 2). In fact, it has been shown that this zone presents significantly larger enzyme immunolocalization and activity levels of PMA than root cap and meristematic zones [37]. The H^+ efflux mediated by PMA is important for the regulation of cytoplasmic pH [10] and the activation of cell wall-loosening enzymes and proteins, both phenomena occurring through acidification of the apoplastic compartment [38]. In agreement with this, we observed a high epidermal cells H^+ efflux in HA-treated roots at elongation/differentiation zone (Figure 3A), leading to an increased capacity of these roots to acidify the local medium (Figure 3B). These effluxes proved to be dependent on PMA, since they were vanadate-sensitive and activated by fusicoccin (data not shown).

In addition, parallel to H^+ efflux, we described for the first time a simultaneous Ca^{+2} influx and anion efflux modulated by HA (Figures 4 and 5). Again, such ionic
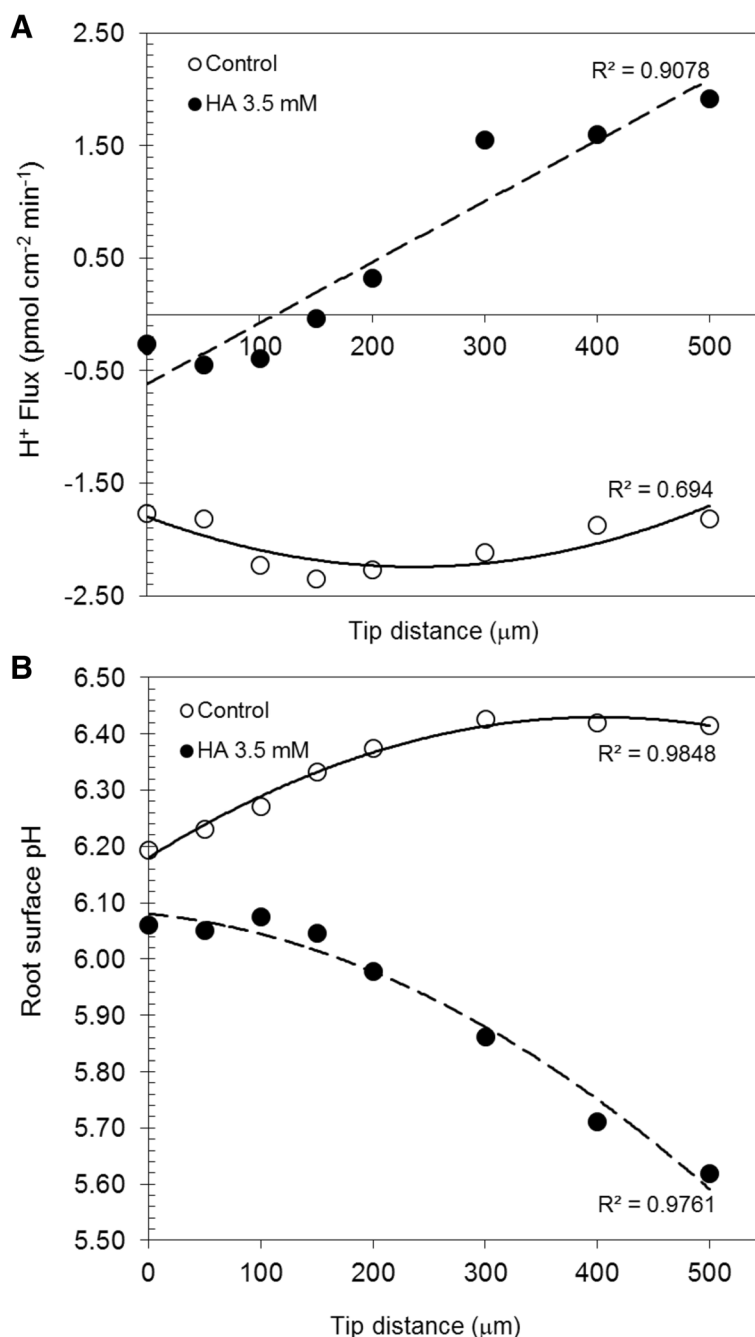
Ramos *et al. Chemical and Biological Technologies in Agriculture* (2015) 2:3

Page 8 of 12

Figure 3 Proton fluxes and surface pH measured along the apical and elongation zones of rice roots. Proton (H^+) fluxes **(A)** and surface pH **(B)** measured along the apical (0 to 100 μm) and elongation (200 to 500 μm) zones of rice roots before (o) and after (●) incubation with 3.5 mM C L^{-1} humic acid (HA).

flux behavior was greater at elongation/differentiation root zone. The relevance of the coordinated spatial bi-directional fluxes for H^+, Ca^{+2}, and anions with HA bio-activity could only be partially explained by the present study, while future attempts using specific probes or in-hibitors for relevant pathways and plant mutagenesis in

some of these functions may better clarify signaling pro-cess related to lateral root induction by HA.

A relationship between proton and anion efflux may be established on the basis of plant nutrition or cytoplasm ionic balance view. Indeed, it is well known that an in-crease in root surface concentration of H^+ generates a

Ramos *et al. Chemical and Biological Technologies in Agriculture* (2015) 2:3
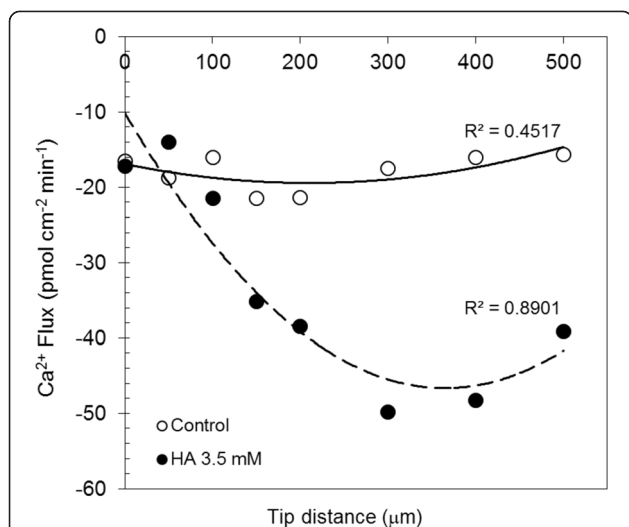
Page 9 of 12

Figure 4 Calcium fluxes in the apical and elongation zones of rice roots. Calcium (Ca^{2+}) fluxes in the apical (0 to 100 μm) and elongation (200 to 500 μm) zones of rice roots, before (○) and after (●) incubation with 3.5 mM C L^{-1} humic acid (HA).

Figure 6 Calcium-dependent protein kinase (CDPK) activity in rice roots treated with and without humic acid. Calcium-dependent protein kinase (CDPK) activity in rice roots treated with and without humic acid (HA: 3.5 mM C L^{-1} and control), respectively. The data represent the mean ± SD ($n = 5$).

proton-motive force that is required to drive the secondary transport of NO_3^-, SO_4^{2-}, Cl^-, Ca^{2+}, and K^+ [10]. It has been reported that the PMA enzyme is stimulated by anions in plant cells [39-41] and host cell-parasite interactions [42]. Therefore, changes in root surface pH are most likely to produce rapid changes in root growth rate [43], thus resulting in rapid volume expansion of nutrient-demand cells followed by symplastic charge balance control.
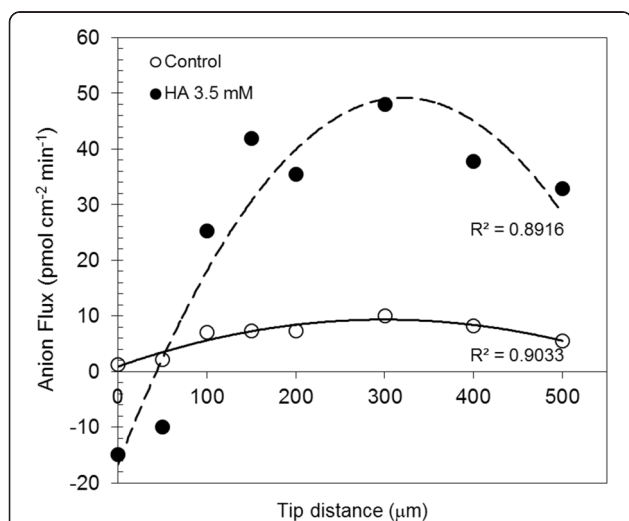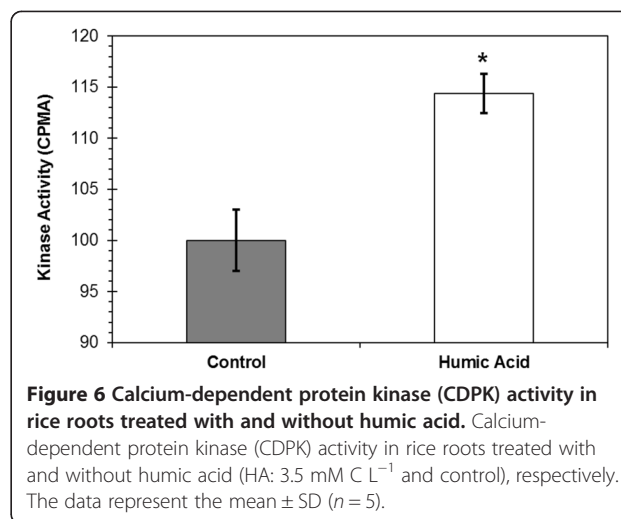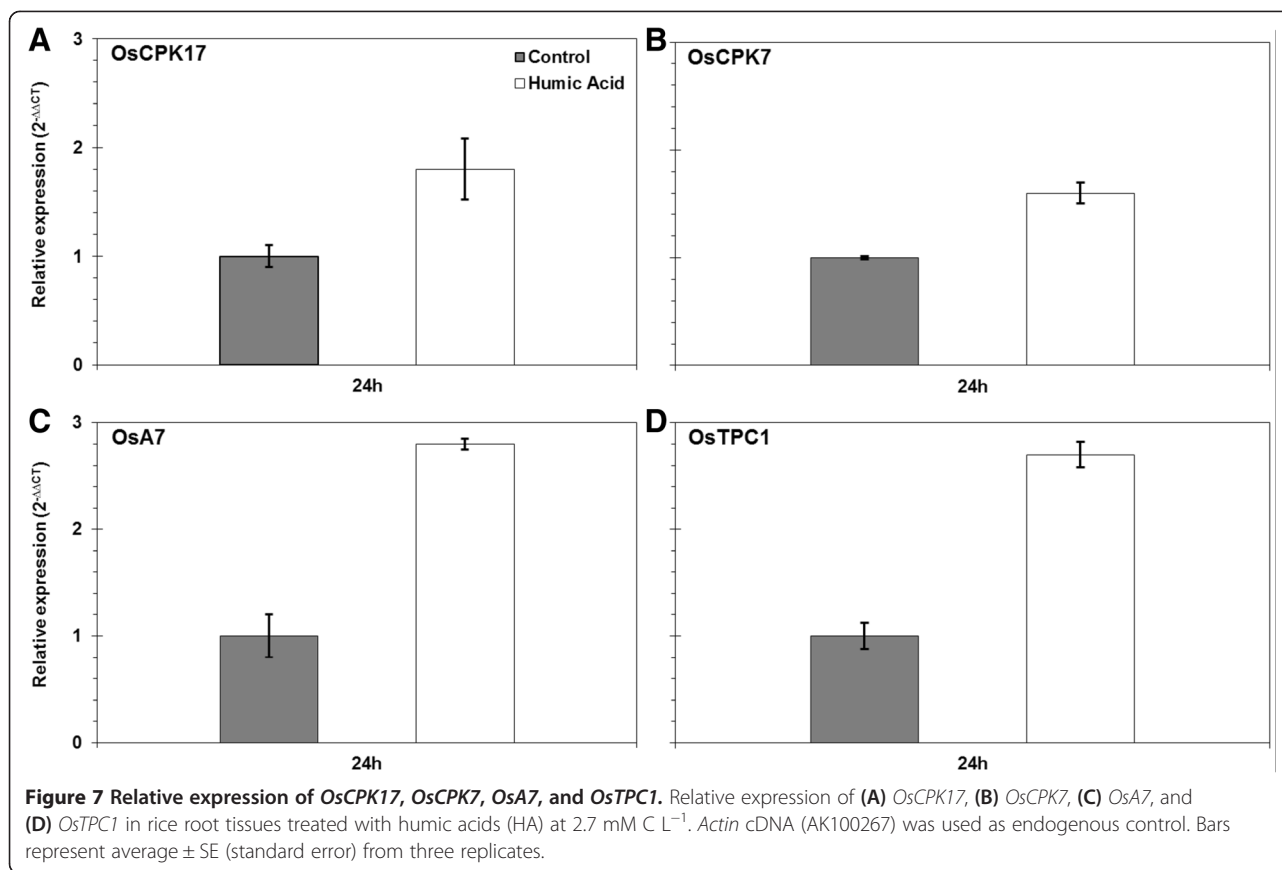

Figure 5 Anion fluxes measurements in the apical and elongation zones of rice roots. Anion fluxes measurements in the apical (0 to 100 μm) and elongation (200 to 500 μm) zones of rice roots, before (○) and after (●) incubation with 3.5 mM C L^{-1} humic acid (HA).

Other candidates that may contribute to the control of extracellular H^+ flux in HA are identified with anions in the growth medium, which are reported to act as stimulators of the PM H^+-ATPase [44]. This effect and the H^+ effluxes are closely related to auxin-induced cell growth, as proposed by the 'acid-growth theory' by Rayle and Cleland [11]. Previous reports described the auxin-like effect of HA using different approaches [7,17,18]. However, changes in organic acid exudation from maize roots induced by HA solutions were previously observed [45]. The relationship between organic acids and proton exudation, earlier described by Ohno et al. [46], was recently observed also by Tomasi et al. [47]. In line with these findings, Puglisi et al. [48] reported an enhancement of organic acid exudation in maize seedlings following a humic matter treatment.

Observed HA-modulated calcium influx (Figure 4) was supposed to be accompanied by an increased Ca-cytosolic concentration, as revealed in this study by both enhanced Ca-transporter and CDPK activity under transcriptional level and biochemical CDPK activity (Figures 6 and 7).

Transient elevations in cytosolic Ca^{2+} concentration are believed to be involved in a multitude of physiological processes, including responses to abiotic stresses, hormones, and pathogens [21]. In the case of HA-treated seedlings, we found a significant increase of Ca^{2+} influx in roots (Figure 4), as well as an enhanced expression of *OsTPC1* voltage-dependent Ca^{2+} channels (Figure 7) that was concomitant to an increased CDPK activity (Figure 6). In fact, it is known that Ca^{2+} channels are known to contribute to short transient Ca^{2+} influx in response to various stimuli, including chilling and microbial interaction [49]. Among the possible effects attributed to the cytosolic increase of Ca^{2+} concentration and down-streaming signaling events, we may include a regulatory H^+ efflux activity in the elongation/differentiation root zone. Indeed,

Ramos *et al. Chemical and Biological Technologies in Agriculture* (2015) 2:3

Page 10 of 12

Figure 7 Relative expression of *OsCPK17*, *OsCPK7*, *OsA7*, and *OsTPC1*. Relative expression of **(A)** *OsCPK17*, **(B)** *OsCPK7*, **(C)** *OsA7*, and **(D)** *OsTPC1* in rice root tissues treated with humic acids (HA) at 2.7 mM C L^{-1}. *Actin* cDNA (AK100267) was used as endogenous control. Bars represent average ± SE (standard error) from three replicates.

H$^+$-ATPase enzyme is stimulated by external anion concentrations [39,40] and inhibited by Ca^{2+} [27]. Hypothetically, during the plant cell cycle, transient cell expansion (growth phase) related to apoplastic proton efflux may be followed by its inhibition by the calcium influx. A cascade signalization of protein-kinase-mediated protein phosphorylation may result in cell and tissue morphogenesis (differentiation phase).

The H$^+$ gradient generated by PMAs provides the energy necessary to drive the secondary transport [16]. Accordingly, we found that the changes in H$^+$ efflux attributable to HA were related to Ca^{2+} influx and anion efflux. However, roots treated with HA displayed strong anion and H$^+$ effluxes primarily at the elongation zone (Figure 3). An explanation may reside in the large net negative charge provided by the HA adsorbed on the root surface, that may be temporarily balanced by PMA activity, thus inducing an anion efflux. In fact, it has been reported that PMA is stimulated by anions in plants [41] and that consequent root surface acidifications are necessary for the mechanism of nutrient uptake [50], as this occurs via PM co-transporters [25]. An increase of PMA activity and extracellular acidification were observed (Figures 2 and 3). The activity of the PM is known to be regulated by reversible protein phosphorylation in a complex manner, including CDPKs [51].

All these observations point toward a role of CDPK during plants response to HA treatments as regulators of PM H$^+$-ATPase. The role of CDPK is remarkable in the context of plant signal transduction. This protein is responsible for post-translational control of target proteins acting as critical regulation of many signaling cascades. Many plant protein kinases act as receptors and participate in processes such as disease resistance, growth development, hormone perception, and stress responses [21]. Increased expression and activity of CDPK in plants treated with HA (Figures 6 and 7) indicate that these proteins can act as elicitors of responses mediated by stress resulting in altered root geometry.

Wan et al. [33] showed a response of many *CDPK* genes under different environmental stress and indentified multiple stress-responsive cis-elements in the promoter region (1 kb) upstream of these genes. Here, we found a concomitant increased expression of *OsTPC1* and *OsCPK7/17* at 24 h after exposure of plants to HA treatment (Figure 7). Correa-Aragunde et al. [52] reported that nitric oxide (NO) mediates auxin lateral root development and the hypothesis of a NO signal downstream of auxin signaling during lateral root formation has been strongly supported [53] and induced by Ca^{2+} waves. Zandonadi et al. [15] showed that maize root architecture is similarly modified by auxin, HA, and sodium

Ramos *et al. Chemical and Biological Technologies in Agriculture* (2015) 2:3

Page 11 of 12

nitroprusside (SNP), thus leading to an increase of lateral root abundance, root density, and PM H^+-ATPase activation.

The role of CDPK, NO, Ca^{2+}, and calmodulin were studied in the auxin-induced adventitious roots in cucumber [54]. It was shown that CDPK was stimulated by auxin and depended on NO, Ca^{2+}, and calmodulin during formation of roots.

The present study suggested a new role for HA-stimulated plant physiology that reveals a potentially important aspect of coevolution between humified organic matter and the plant growth and development. Changing the ion fluxes across the root plasma membrane implies modifications in transmembrane electrical potential. The latter is generated by the electrogenic H^+ pumps involved in the ion transport systems as well as by the signal transduction related to root morphogenesis.

Conclusions

Humic matter acts a plant elicitor by triggering a series of cell signaling events. Our results suggest a model for cell signaling in roots that is directly linked to nutrient uptake and lateral root emergence. We have shown that HA induce a positive modulation of PM H^+-ATPase activity and expression that controls the H^+ efflux, root surface pH, and consequently triggers modifications in the anion fluxes. This hyperpolarization, in turn, induces a pH signal that modulates Ca^{2+} transport by increasing cytosolic free Ca^{2+} concentration, which then acts as a second messenger though the mediation of a variety of cellular responses like CDPK activities and anion channel activation. A large anion efflux is activated by the HA negative charges which are built up on the root surface and re-induce H^+-ATPase activity. Within the effort to elucidate the complex HA-plant response mechanism, our results show that HA have an effect on various entry points of the cell signaling machinery, such as fluxes of H^+ and Ca^{2+}, H^+-ATPase and CDPK activity, as well as the expression of Ca^{2+} transporters. Overall, our findings of this work indicate that plant nutrient uptake and growth promotion mediated by humic matter may consist in a pH-dependent phenomenon.

Additional files

Additional file 1: Table S1. Gene-specific primers for real-time PCR.
Additional file 2: Figure S1. CP/MAS ^{13}C NMR spectra of humic acids.

Competing interests
The authors declare that they have no competing interests.

Authors' contributions
ACR carried out the ion flux measurement and drafted the manuscript. LBD carried out the CDPK activity and drafted the manuscript. LAS and MSF carried out the molecular genetic studies and drafted the manuscript.

NOA did the humic acid characterization. FLO and LPC conceived of the study and participated in its design and coordination and helped to draft the manuscript. All authors read and approved the final manuscript.

Author details
[1]Laboratório de Bioquímica e Fisiologia de Microrganismos, Universidade Estadual do Norte Fluminense Darcy Ribeiro (UENF), Av. Alberto Lamego 2000, Campos dos Goytacazes 28013-602, Brazil. [2]Laboratório de Microbiologia Ambiental e Biotecnologia, Universidade de Vila Velha (UVV), Rua Comissário José Dantas de Melo 21, Boa Vista, Vila Velha, Espírito Santo, Brazil. [3]Departamento de Solos da Universidade Federal Rural do Rio de Janeiro (UFRRJ), Seropédica, km 7 BR 465, Seropédica, Rio de Janeiro CEP 23851-970, Brazil. [4]Universidade Estadual do Norte Fluminense Darcy Ribeiro (UENF) Núcleo de Desenvolvimento de Insumos Biológicos para Agricultura (NUDIBA), Av. Alberto Lamego 2000, Campos dos Goytacazes 28013-602, Brazil.

References
1. Orsi M (2014) Molecular dynamics simulation of humic substances. Chem Biol Technol Agr 1:10
2. Nardi S, Carletti P, Pizzeghello D, Muscolo A (2009) Biological activities of humic substances. In Senesi N,Xing B Huang PM (ed) Biophysico-Chemical Processes Involving Natural Non Living Organic Matter in Environmental Systems. Vol 2, part 1: fundamentals and impact of mineral-organic biota interactions on the formation, transformation. Turnover and storage of natural nonliving organic matter (NOM). Wiley, Hoboken, pp305-340
3. Canellas LP, Olivares FL (2014) Physiological responses to humic substances as plant growth promoter. Chem Biol Technol Agr 1:3
4. Mora V, Bacaicoa E, Zamarreño AM, Agguirre E, Garnica M, Fuentes M, García-Mina JM (2010) Action of humic acid on promotion of cucumber shoot growth involves nitrate-related changes associated with the root-to-shoot distribution of cytokinins, polyamines and mineral nutrients. J Plant Physiol 167:633–642
5. Canellas LP, Dobbss LB, Oliveira AL, Chagas JG, Aguiar NO, Rumjanek VM, Novotny EH, Olivares FL, Spaccini R, Piccolo A (2012) Chemical properties of humic matter as related to induction of plant lateral roots. Eur J Soil Sci 63:315–324
6. Mora V, Bacaicoa E, Baigorri R, Zamarreño AM, García-Mina JM (2014) NO and IAA key regulators in the shoot growth promoting action of humic acid in *Cucumis sativus* L. J Plant Growth Regul 33:430–439
7. Dobbss LB, Canellas LP, Olivares FL, Aguiar NO, Peres LEP, Azevedo M, Spaccini R, Piccolo A, Façanha AR (2010) Bioactivity of chemically transformed humic matter from vermicompost on plant root growth. J Agr Food Chem 58:3681–3688
8. Feijó JA, Sainhas J, Hackett GR, Kunkel JG, Hepler PK (1999) Growing pollen tubes posses a constitutive alkaline band in the clear zone and a growth-dependent acidic tip. J Cell Biol 144:483–496
9. Konrad KR, Wudick MM, Feijó JA (2012) Calcium regulation of tip growth: new genes for old mechanisms. Curr Opin Plant Biol 14:721–730
10. Felle HH (2001) pH: signal and messenger in plant cells. Plant Biol 3:577–591
11. Rayle DL, Cleland RE (1992) The acid growth theory of auxin-induced cell elongation is alive and well. Plant Physiol 99:1271–1274
12. Rober-Kleber N, Albrechtová JTP, Fleig S, Huck N, Michalke W, Wagner E, Speth V, Neuhaus G, Fischer-Iglesias C (2003) Plasma membrane H^+-ATPase is involved in auxin-mediated cell elongation during wheat embryo development. Plant Physiol 131:1302–1312
13. Fasano JM, Swanson SJ, Blancaflor EB, Dowd PE, Kao T, Gilroy S (2001) Changes in root cap pH are required for the gravity response of the *Arabidopsis* root. Plant Cell 13:907–92
14. Trevisan S, Pizzeghello D, Ruperti B, Francioso O, Sassi A, Palme K, Quaggiotti S, Nardi S (2010) Humic substances induce lateral root formation

Ramos *et al. Chemical and Biological Technologies in Agriculture* (2015) 2:3

Page 12 of 12

and expression of the early auxin-responsive IAA19 gene and DR5 synthetic element in *Arabidopsis*. Plant Biol 12:604–614

15. Zandonadi DB, Santos MP, Dobbss LB, Olivares FL, Canellas LP, Binzel ML, Okorokova-Façanha AL, Façanha AR (2010) Nitric oxide mediates humic acids-induced root development and plasma membrane H$^+$-ATPase activation. Planta 231:1025–1036

16. Palmgren MG (2001) Plant plasma membrane H$^+$-ATPases: powerhouses for nutrient uptake. Annl Rev Plant PhysiolPlant Mol Biol 52:817–845

17. Canellas LP, Façanha AO, Olivares FL, Façanha AR (2002) Humic acids isolated from earthworm compost enhance root elongation, lateral root emergence, and plasma membrane H$^+$-ATPase activity in maize roots. Plant Physiol 130:1951–1957

18. Quaggiotti S, Rupert B, Pizzeghello D, Francioso O, Tugnoli V, Nardi S (2004) Effect of low molecular size humic substances on nitrate uptake and expression of genes involved in nitrate transport in maize (*Zea mays* L.). J Exp Bot 55:803–813

19. Salomon D, Bonshtien A, Sessa G (2009) A chemical-genetic approach for functional analysis of plant protein kinases. Plant Signal Behav 4:645–647

20. Zhang Y, Gao P, Yuan JS (2010) Plant protein-protein interaction network and 58. Interactome Curr Genomics 11:40–46

21. Kudla J, Batistic O, Hashimoto K (2010) Calcium signals: the lead currency of plant information processing. Plant Cell 22:541–563

22. Hamada H, Kurusu T, Okuma E, Nokajima H, Kiyoduka M, Koyano T, Sugiyama Y, Okada K, Koga J, Saji H, Miyao A, Hirochika H, Yamane H, Murata Y, Kuchitsu K (2012) Regulation of a proteinaceous elicitor-induced Ca^{2+} influx and production of phytoalexins by a putative voltage-gated cation channel, OsTPC1, in cultured rice cells. J Biol Chem 23:9931–0039

23. Pei ZM, Murata Y, Benning G, Thomine S, Klusener B, Allen GJ, Grill E, Schroeder JI (2000) Calcium channels activated by hydrogen peroxide mediate abscisic acid signalling in guard cells. Nature 406:731–734

24. Lowry OH, Rosebrough NJ, Farr AL, Randall RJ (1951) Protein measurement with the Folin phenol reagent. J Biol Chem 193:265–275

25. Ramos AC, Façanha AR, Lima PT, Feijó JA (2008) pH signature for the responses of arbuscular mycorrhizal fungi to external stimuli. Plant SignalBehav 3:850–852

26. Ramos AC, Lima PT, Dias PN, Kasuya MCM, Feijó JA (2009) A pH signaling mechanism involved in the spatial distribution of calcium and anion fluxes in ectomycorrhizal roots. New Phytol 181:448–462

27. Lino B, Baizabal-Aguirre VM, González de la Vara LE (1998) The plasma-membrane H$^+$-ATPase from beet root is inhibited by a calcium-dependent phosphorylation. Planta 204:352–359

28. Gao J, Liu J, Li B, Li Z (2001) Isolation and purification of functional total RNA from blue-grained wheat endosperm tissues containing high levels of starches and flavonoids. Plant Mol Biol Rep 19:185–1185

29. Sperandio MVL, Santos LA, Bucher CA, Fernandes MS, Souza SR (2011) Isoforms of plasma membrane H + -ATPase in rice root and shoot are differentially induced by starvation and resupply of NO$_3^-$ or NH$_4^+$. Plant Sci 180:251–258

30. Livak KJ, Schmittgen TD (2001) Analysis of relative gene expression data using real-time quantitative PCR and the 2 − ΔΔCt method. Methods 25:402–408

31. Kurusu T, Sakurai Y, Miyao A, Hirochika H, Kuchitsu K (2004) Identification of a putative voltage-gated Ca^{2+}-permeable channel (OsTPC1) involved in Ca^{2+} influx and regulation of growth and development in rice. Plant Cell Physiol 45:693–702

32. Arango M, Gevaudant F, Oufattole M, Boutry M (2003) The plasma membrane proton pump ATPase: the significance of gene subfamilies. Planta 216:355–365

33. Wan B, Lin Y, Mou T (2007) Expression of rice Ca^{2+}-dependent protein kinases (CDPKs) genes under different environmental stresses. FEBS Lett 581:1179–1189

34. Akimoto-Tomiyama C, Sakata K, Yazaki J, Nakamura K, Fujii F (2003) Rice gene expression in response to Nacetylchitooligosaccharide elicitor: comprehensive analysis by DNA microarray with randomly selected ESTs. Plant Mol Biol 52:537–551

35. Abbasi F, Onodera H, Toki S, Tanaka H, Komatsu S (2004) *OsCDPK13*, a calcium-dependent protein kinase gene from rice, is induced by cold and gibberellin in rice leaf sheath. Plant Mol Biol 55:541–552

36. Aguiar NO, Novotny EH, Oliveira AL, Rumjanek VM, Olivares FL, Canellas LP (2013) Prediction of humic acids bioactivity using spectroscopy and multivariate analysis. J Geochem Explor 129:95–102

37. Enriquez-Arredondo C, Sanchez-Nieto S, Rendon-Huerta E, Gonzalez-Halphen D, Gavilanes-Ruiz M, Diaz-Pontones D (2005) The plasma membrane H$^+$-ATPase of maize embryos localizes in regions that are critical during the onset of germination. Plant Sci 169:11–19

38. Hager A (2003) Role of the plasma membrane H$^+$-ATPase in auxin induced elongation growth. Historical and new aspects. J Plant Res 116:483–505

39. Churchill KA, Sze H (1984) Anion-sensitive, H$^+$ pumping ATPase of oat roots: direct effects of Cl$^-$, NO$_3^-$ and a disulfonic stilbene. Plant Physiol 76:490–497

40. Ullrich CI, Novacky AJ (1990) Extra- and intracellular pH and membrane potential changes induced by K+, Cl−, H2PO4-, NO3-, uptake and fusicoccin in root hairs of Limnobium storoniferum. Plant Physiol 94:1561–1567

41. Zimmermann S, Thomine S, Guern J, Barbier-Brygoo H (1994) An anion current at the plasma membrane of tobacco protoplasts is ATP-dependent voltage regulation and is modulated by auxin. Plant J 6:707–716

42. Vieira L, Slotki I, Cabantchik ZI (1995) Chloride conductive pathways which support electrogenic H$^+$ pumping by *Leishmania major* Promastigotes. J Biol Chem 270:5299–5304

43. Peters WS, Felle HH (1999) The correlation of profiles of surface pH and elongation growth in maize roots. Plant Physiol 121:905–912

44. Garnett TP, Shabala SN, Smethurst PJ, Newman IA (2001) Kinetics of ammonium and nitrate uptake by eucalypt roots and associated proton fluxes measured using ion selective microelectrodes. Funct Plant Biol 30:1165–1176

45. Canellas LP, Teixeira Junior LRL, Dobbss LB, Silva CA, Médici LO, Zandonadi DB, Façanha AR (2008) Humic acids cross interactions with root and organic acids. Ann Appl Biol 153:157–166

46. Ohno T, Nakahira S, Suzuki Y, Kani T, Hara T, Koyama H (2004) Molecular characterization of plasma membrane H$^+$ATPase in a carrot mutant cell line with enhanced citrate excretion. Plant Physiol 122:265–274

47. Tomasi N, Kretzschmar T, Espen L, Weisskopf L, Thoe Fuglsang A, Palmgren G, Neumann G, Varanini Z, Pinton R, Martinoia E, Cesco E (2009) Plasma membrane H$^+$ATPase-dependent citrate exudation from cluster roots of phosphate-deficient white lupin. Plant Cell Environ 32:465–475

48. Puglisi E, Fragoulis G, Del Re AM, Spaccini R, Gigliotti G, Said-Pullicino D, Trevisan M (2008) Carbon deposition in soil rhizosphere following amendments with soluble fractions, as evaluated by combined soil-plant rhizobox and reporter gene systems. Chemosphere 73:1292–1299

49. Thion L, Mazars C, Nacry P, Bouchez D, Moreau M, Ranjeva R, Thuleau P (1998) Plasma membrane depolarizationactivated depolarizationactivated calcium channels, stimulated by microtubule-depolymerizing drugs in wild-type Arabidopsis thaliana protoplasts, display constitutively large activities and a longer half-life in ton 2 mutant cells affected in the organization of cortical microtubules. Plant J 13:603–610

50. Forde BG (2000) Nitrate transporters in plants: structure, function and regulation. *v.* Biochim Biophys Acta 1465:219–235

51. Vera-Estrella R, Barkla BJ, Higgins VJ, Blumwald E (1994) Plant defense response to funga1 pathogens. Activation of host-plasma membrane H$^+$-ATPase by elicitor-induced enzyme dephosphorylation. Plant Physiol 104:209–215

52. Correa-Aragunde N, Graziano M, Lamattina L (2004) Nitric oxide plays a central role in determining lateral root development in tomato. Planta 218:900–905

53. Kolbert Z, Bartha B, Erdei L (2008) Exogenous auxin-induced NO synthesis is nitrate reductase-associated in *Arabidopsis thaliana* root primordia. J Plant Physiol 165:967–975

54. Lanteri ML, Pagnussat GC, Lamattina L (2006) Calcium and calcium-dependent protein kinases are involved in nitric oxide- and auxin-induced adventitious root formation in cucumber. J Exp Bot 57:1341–1351